SLAC-PUB-7732
January 1998

High Energy Photon-Photon and Electron-Photon Collisions *

Stanley J. Brodsky

Stanford Linear Accelerator Center,
Stanford University, Stanford, California 94309

Abstract

The advent of a next linear $e^{\pm}e^{-}$ collider and back-scatterd laser beams will allow the study of a vast array of high energy processes of the Standard Model through the fusion of real and virtual photons and other gauge bosons. As examples, I discuss virtual photon scattering $\gamma^*\gamma^* \to X$ in the region dominated by BFKL hard Pomeron exchange and report the predicted cross sections at present and future $e^{\pm}e^{-}$ colliders. I also discuss exclusive $\gamma\gamma$ reactions in QCD as a measure of hadron distribution amplitudes and a new method for measuring the anomalous magnetic and quadrupole moments of the W and Z gauge bosons to high precision in polarized electron-photon collisions.

Presented at e-e-97
2nd International Workshop on
Electron-Electron Interactions at TeV Energies
University of California, Santa Cruz
September 22–24, 1997

*Work supported by the Department of Energy, contract DE–AC03–76SF00515.

HIGH ENERGY PHOTON-PHOTON AND ELECTRON-PHOTON COLLISIONS *

STANLEY J. BRODSKY

Stanford Linear Accelerator Center
Stanford University, Stanford, California 94309

The advent of a next linear $e^{\pm}e^{-}$ collider and back-scatterd laser beams will allow the study of a vast array of high energy processes of the Standard Model through the fusion of real and virtual photons and other gauge bosons. As examples, I discuss virtual photon scattering $\gamma^*\gamma^* \to X$ in the region dominated by BFKL hard Pomeron exchange and report the predicted cross sections at present and future $e^{\pm}e^{-}$ colliders. I also discuss exclusive $\gamma\gamma$ reactions in QCD as a measure of hadron distribution amplitudes and a new method for measuring the anomalous magnetic and quadrupole moments of the W and Z gauge bosons to high precision in polarized electron-photon collisions.

1. Introduction

The largest production rates at a high energy $e^{\pm}e^{-}$ collider arise from photon-photon fusion processes $ee \to ee\gamma\gamma \to eeX$ since the cross sections increase logarithmically with the available energy.[1] The final state X can be hadrons, leptons, gauge bosons, and any other $C = +$ state coupling to the electromagnetic current. At very high energies the fusion of any pair of gauge bosons $\gamma, Z^0, W^{\pm}$ becomes accessible. The final-state leptons in $ee \to eeX$ can be tagged to provide a source of virtual photons or Z^0 bosons of tuneable energy and virtuality. In addition, by the use of laser beams backscattering on a polarized electron beam, one can obtain remarkably high luminosities for high energy polarized real photon $\gamma\gamma$ and γe collisions.[2] Such collisions will open up a large array of important tests of the Standard Model as well as discovery tools for new particles.

In this talk I will focus on three important areas of physics involving high energy real and virtual photon beams: (a) exclusive two photon processes as a study of hadron structure in QCD, (b) the study of the total virtual photon-photon scattering cross section as a definitive probs of the hard QCD (BFKL) pomeron; and (c) the study of of polarized-photon polarized-electron collisions in the process $\gamma e^{-} \to W\nu$ as a high precision test of the Standard model. The latter reaction is particularly

*Work supported by the Department of Energy under contract number DE–AC03–76SF00515.

well-matched to a high lumionosity polarized electron-electron and backscattered laser beam facility at the next linear collider. High energy photon-photon collisions also open up a huge range of novel QCD studies, such as measurements of the photon structure function, the search for $C = -1$ odderon exchange in exclusive reactions such as $\gamma\gamma \to \pi^0\pi^0$ at $s \gg -t$, and gluon jet studies in inclusive reactions such as $\gamma\gamma \to gg$.

2. Exclusive Photon-Photon Reactions

Exclusive $\gamma\gamma \to$ hadron pairs are among the most fundamental processes in QCD, providing a detailed examination of Compton scattering in the crossed channel. In the high momentum transfer domain ($s, t,$ large, θ_{cm} for t/s fixed), these processes can be computed from first principles in QCD, yielding important information on the nature of the QCD coupling α_s and the form of hadron distribution amplitudes. Similarly, the transition form factors $\gamma^*\gamma$, $\gamma^*\gamma \to \pi^0, \eta^0, \eta', \eta_c \ldots$ provide rigorous tests of QCD and definitive determinations of the meson distribution amplitudes $\phi_H(x, Q)$.[3]

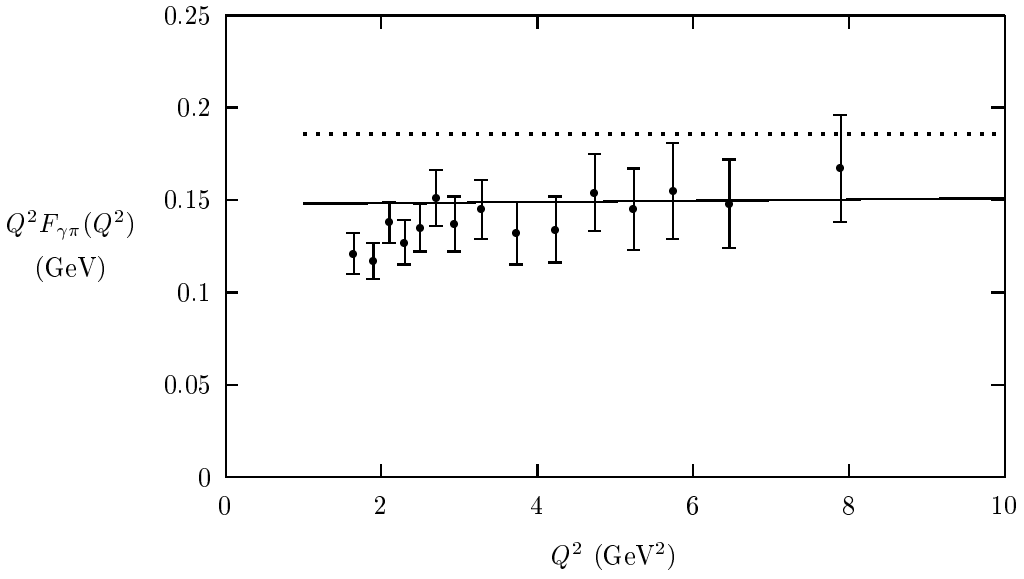

Figure 1: The $\gamma \to \pi^0$ transition form factor. The solid line is the full prediction including the QCD correction; the dotted line is the LO prediction $Q^2 F_{\gamma\pi}(Q^2) = 2f_\pi$.

The simplest hadronic exclusive reaction is the $\gamma e \to e'\pi^0$ process which measures the $\gamma \to \pi^0$ transition form factor. The present data from CLEO shown in figure (1) shows remarkable consistency with the next-to-leading-order (NLO) leading-twist scaling QCD predictions [3,4] for photon virtualities up to $Q^2 = 8$

GeV^2. See Fig. (1). The consistency of the CLEO data [5] with the predicted normalization and the apparent absence of violations of leading-twist scaling requires that the basic wavefunction which describes the momentum distribution in the valence $q\overline{q}$ Fock state of the pion, the pion distribution amplitude, has the form $\phi(x,Q) = \sqrt{3} f_\pi x(1-x)$, which is the asymptotic leading anomalous dimension solution to the QCD evolution equation for the meson light-cone wavefunction. It also assumes that the running coupling which appears in the NLO corrections is slowly varying at small momentum transfer.[6]

Since the cross section of the single meson exclusive reaction falls off as only one power of Q^2 compared to scale-invariant reactions, studies of the normalization and scaling of other $\gamma e \to e' M^0$ reactions should be practical for general $C = +$ neutral mesons including the η_c and η_b at high photon virtuality Q^2 in high energy γe collisions. Such measurements can provide fundamental information on the nature of the hadron wavefunctions and their anomalous dimensions. Further discussion of the theory of exclusive single hadron and hadron pair production in $\gamma\gamma$ and $e\gamma$ collisions can be found in a recent paper by Ji, Robertson, Pang and myself.[6]

3. Probing the Hard QCD Pomeron in Virtual Photon Collisions

The BFKL equation describes scattering processes in QCD in the limit of large energies and fixed (sufficiently large) momentum transfers. The study discussed in this section analyzes the prospects for using virtual photon-photon collisions at LEPII and a next linear collider as a probe of QCD dynamics in this region.[7,8] The quantity we focus on is the total cross section for scattering two photons sufficiently far off shell at large center-of-mass energies, $\gamma^*(Q_A^2) + \gamma^*(Q_B^2) \to$ hadrons, $s \gg Q_A^2, Q_B^2 \gg \Lambda_{QCD}^2$. This process can be observed at high-energy and high-luminosity $e^\pm e^-$ colliders as well as $\mu^\pm \mu^-$ colliders, where the photons are produced from the lepton beams by bremsstrahlung. The $\gamma^*\gamma^*$ cross section can be measured in collisions in which both the outgoing leptons are tagged.

The basic motivation for this study is that compared to tests of BFKL dynamics in deeply inelastic lepton-hadron scattering (see, for instance, the review by Abramowicz [9]) the off-shell photon cross section presents an essential theoretical advantage because it does not involve a non-perturbative target. The photons act as color dipoles with small transverse size, so that the QCD interactions can be treated in a fully perturbative framework.

The structure of $\gamma^*\gamma^*$ high-energy scattering is shown schematically in Fig. (2). We work in a frame in which the photons q_A, q_B have zero transverse momenta and are boosted along the positive and negative light-cone directions. In the leading logarithm approximation, the process can be described as the interaction of two $q\overline{q}$ pairs scattering off each other via multiple gluon exchange. The $q\overline{q}$ pairs are in a color-singlet state and interact through their color dipole moments. The gluonic function $\mathcal{F}$ is obtained from the solution to the BFKL equation.[10]

The analysis of the transverse-distance scales involved in the scattering illus-

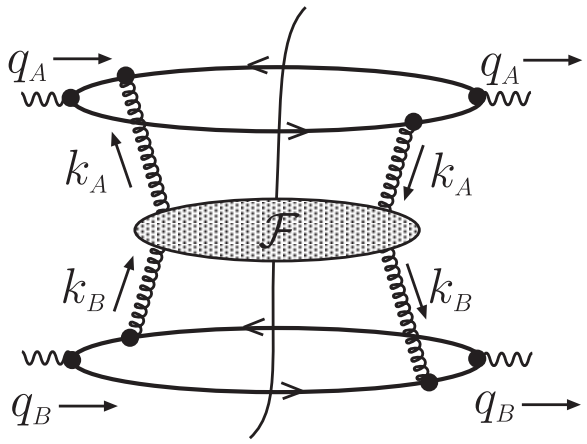

Figure 2: The virtual photon cross section in the high energy limit.

trates a few distinctive features of this process. The mean transverse size of each $q\overline{q}$ dipole is given, in the first approximation, by the reciprocal of the corresponding photon virtuality:

$$< R_{\perp A} > \sim 1/Q_A \quad , \qquad < R_{\perp B} > \sim 1/Q_B \qquad . \tag{1}$$

However, fluctuations can bring in much larger transverse sizes. Large-size fluctuations occur as a result of the configurations in which one quark of the pair carries small transverse momentum and a small fraction of the photon longitudinal momentum (the so-called aligned-jet configurations [11]) . For example, for the momentum p_A of the quark created by photon A:

$$\mathbf{p}_{\perp A} \ll Q_A \quad , \qquad z_A \equiv p_A^+/q_A^+ \ll 1 \qquad . \tag{2}$$

The actual size up to which the $q\overline{q}$ pair can fluctuate is controlled by the scale of the system that it scatters off. Therefore, in $\gamma^*\gamma^*$ scattering the fluctuations in the transverse size of each pair are suppressed by the off-shellness of the photon creating the other pair. If *both* photons are sufficiently far off shell, the transverse separation in each $q\overline{q}$ dipole stays small.[7] This can be contrasted with the case of deeply inelastic $e\,p$ scattering (or $e\,\gamma$, where γ is a (quasi-)real photon). In this case, the $q\overline{q}$ pair produced by the virtual photon can fluctuate up to sizes of the order of a hadronic scale, that is, $1/\Lambda_{QCD}$. This results in the deeply inelastic cross section being determined by an interplay of short and long distances.

In principle, the $q\overline{q}$ dipoles in the $\gamma^*\gamma^*$ process could still fluctuate to bigger sizes in correspondence of configurations in which the jet alignment occurs twice, once for each photon. However, such configurations cost an extra overall power of $1/Q^2$

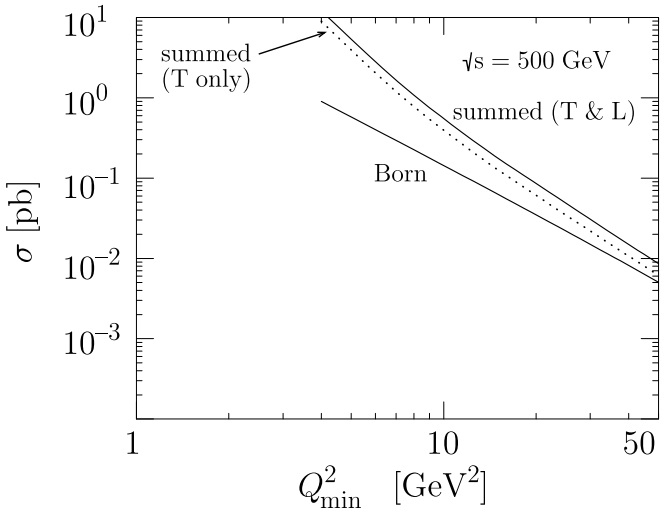

Figure 3: The $Q^2_{\rm min}$ dependence of the e^+e^- integrated rate for $\sqrt{s} = 500$ GeV. The choice of the cuts and of the scales in the leading logarithm result is as in Brodsky *et al.*[7] The dot-dashed and solid lines correspond to the result of using, respectively, the Born and the BFKL-summed expressions for the photon-photon cross section. The dotted curve shows the contribution to the summed result coming from transversely polarized photons.

in the cross section (terms proportional to $1/(Q_A^2\, Q_B^2)$ rather than $1/(Q_A\, Q_B)$).[12] Therefore, they only contribute at the level of sub-leading power corrections to $\sigma(\gamma^*\gamma^*)$.

Even though the $q\overline{q}$ dipoles have small transverse size, sensitivity to large transverse distances may be brought in through the BFKL function $\mathcal{F}$. This indeed is expected to occur when the energy s becomes very large. As s increases, the typical impact parameters dominating the cross section for BFKL exchange grow to be much larger than the size of the colliding objects.[13] One can interpret this as providing an upper bound on the range of values of $\left(\alpha_s(Q^2)\, \ln(s/Q^2)\right)$ in which the simple BFKL approach to virtual photon scattering is expected to give reliable predictions.[7]

The calculation of $\sigma(\gamma^*\gamma^*)$ and the form of the result are discussed in detail in recent papers.[7,8]. We recall here the main features:

i) for large virtualities, $\sigma(\gamma^*\gamma^*)$ scales like $1/Q^2$, where $Q^2 \sim \max\{Q_A^2, Q_B^2\}$. This is characteristic of the perturbative QCD prediction. Models based on Regge factorization (which work well in the soft-interaction regime dominating $\gamma\,\gamma$ scattering near the mass shell) would predict a higher power in $1/Q$.

ii) $\sigma(\gamma^*\gamma^*)$ is affected by logarithmic corrections in the energy s to all orders in

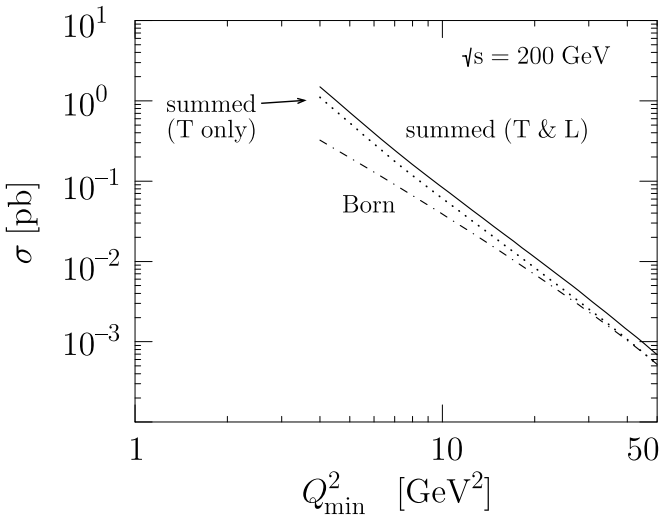

Figure 4: Same as in Fig. 3 for $\sqrt{s} = 200$ GeV.

α_s. As a result of the BFKL summation of these contributions, the cross section rises like a power in s, $\sigma \propto s^\lambda$. The Born approximation to this result (that is, the $\mathcal{O}(\alpha_s^2)$ contribution, corresponding to single gluon exchange in the graph of Fig. 2) gives a constant cross section, $\sigma_{Born} \propto s^0$. This behavior in s can be compared with lower-order calculations which do not include the corrections associated to (single or multiple) gluon exchange. Such calculations would give cross sections that fall off like $1/s$ at large s.

These features are reflected at the level of the $e^\pm e^-$ scattering process. The $e^\pm e^-$ cross section is obtained by folding $\sigma(\gamma^*\gamma^*)$ with the flux of photons from each lepton. In Figs. 3 and 4, we integrate this cross section with a lower cut on the photon virtualities (in order that the coupling α_s be small, and that the process be dominated by the perturbative contribution) and a lower cut on the photon-photon c.m.s. energy (in order that the high energy approximation be valid). We plot the result as a function of the lower bound $Q^2_{\rm min}$, illustrating the expected dependence of the photon-photon cross section on the photon virtualities. Figure 3 is for the energy of a future $e^\pm e^-$ collider. Figure 4 refers to the LEP collider operating at $\sqrt{s} = 200$ GeV. Details on our choice of cuts may be found in my paper with Hautmann and Soper, *et al.*[7]

From Figs. 3 and 4, for a value of the cut $Q_{\rm min} = 2$ GeV we find $\sigma \simeq 1.5\,{\rm pb}$ at LEP200 energies, and $\sigma \simeq 12\,{\rm pb}$ at the energy of a future collider. These cross sections would give rise to about 750 events at LEP200 for a value of the luminosity $L = 500\,{\rm pb}^{-1}$, and about 6×10^5 events at $\sqrt{s} = 500$ GeV for $L = 50\,{\rm fb}^{-1}$. The above value of $Q_{\rm min}$ would imply detecting leptons scattered through angles down

to about 20 mrad at LEP200, and about 8 mrad at a future 500 GeV collider. If instead we take, for instance, $Q_{\rm min} = 6$ GeV, the minimum angle at a 500 GeV collider is 24 mrad. Then the cross section is about 2×10^{-2} pb, corresponding to about 10^3 events. The dependence on the photon-photon c.m. energy $\sqrt{\hat{s}}$ can be best studied by fixing $Q_{\rm min}$ and looking at the cross section $d\sigma/(d\ln\hat{s}\,dy)$ (here y is the photon-photon rapidity). In Figure 5 we plot this cross section at $y = 0$. While at the lowest end of the range in $\sqrt{\hat{s}}$ the curves are strongly dependent on the choice of the cuts, for increasing $\sqrt{\hat{s}}$ the plotted distribution is rather directly related to the behavior of $\sigma(\gamma^*\gamma^*)$ discussed earlier. In particular, as $\sqrt{\hat{s}}$ increases to about 100 GeV we see the Born result flatten out and the summed BFKL result rise, while the contribution from quark exchange is comparatively suppressed. The damping towards the higher end of the range in $\sqrt{\hat{s}}$ affects all curves and is due to the influence of the photon flux factors.

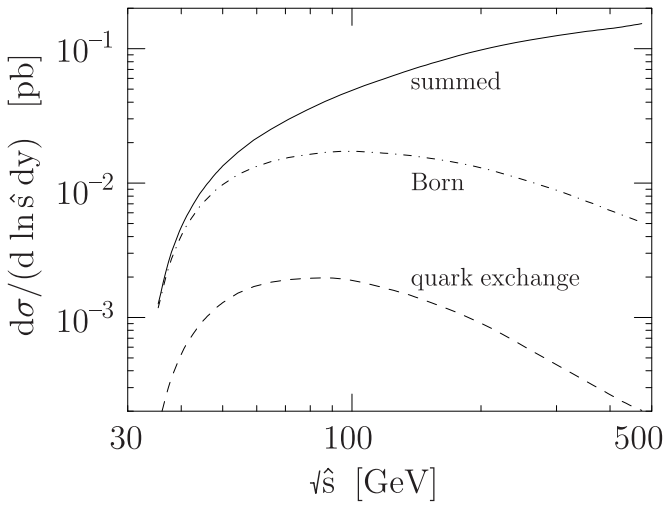

Figure 5: The cross section $d\sigma/(d\ln\hat{s}\,dy)$ at $y = 0$ for $\sqrt{s} = 500$ GeV. We take $Q^2_{\rm min} = 10$ GeV^2. The solid curve is the summed BFKL result. The dot-dashed curve is the Born result. The dashed curve shows the (purely electromagnetic) contribution arising from the scattering of (transversely polarized) photons via quark exchange.

Figure 5 is computed for $\sqrt{s} = 500$ GeV. The corresponding curves at LEP200 energies are qualitatively similar. The main difference is that at $\sqrt{s} = 200$ GeV there is less available range for $\sqrt{\hat{s}}$.

We see from the results presented above that at a future $e^{\pm}e^-$ collider it should be possible to probe the effects of pomeron exchange in a range of Q^2 where summed

perturbation theory applies. One should be able to investigate this region in detail by varying Q_A, Q_B and $\hat{s}$ independently. At LEP200 such studies appear to be more problematic mainly because of limitations in luminosity. Even with a modest luminosity, however, one can access the region of relatively low Q^2 if one can get down to small enough angles. This would allow one to examine experimentally the transition between soft and hard scattering.

4. Precision limits on Anomalous Couplings of the W and Z[14]

The Dirac value $g = 2$ for the magnetic moment $\mu = geS/2M$ of a particle of charge e, mass M, and spin S, plays a special role in quantum field theory. As shown by Weinberg [15] and Ferrara *et. al* [16], the canonical value $g = 2$ gives an effective Lagrangian which has maximally convergent high energy behavior for fields of any spin. In the case of the Standard Model, the anomalous magnetic moments $\mu_a = (g-2)eS/2M$ and anomalous quadrupole moments $Q_a = Q + e/M^2$ of the fundamental fields vanish at tree level, ensuring a quantum field theory which is perturbatively renormalizable. However, as one can use the DHG sum rule [17] to show that the magnetic and quadrupole moments of spin-$\frac{1}{2}$ or spin-1 bound states approach the canonical values $\mu = eS/M$ and $Q = -e/M^2$ in the zero radius limit $MR \to 0$ [18,19,20], independent of the internal dynamics. Deviations from the predicted values will thus reflect new physics and interactions such as virtual corrections from supersymmetry or an underlying composite structure.

The canonical values $g = 2$ and $Q = -e/M^2$ lead to a number of important phenomenological consequences: (1) The magnetic moment of a particle with $g = 2$ processes with the same frequency as the Larmor frequency in a constant magnetic field. This synchronicity is a consequence of the fact that the electromagnetic spin currents can be formally generated by an infinitesimal Lorentz transformation. [21,22] (2) The forward helicity-flip Compton amplitude for a target with $g = 2$ vanishes at zero energy. [23] (3) The Born amplitude for a photon radiated in the scattering of any number of incoming and outgoing particles with charge e_i and four-momentum p_i^μ vanishes at the kinematic angle where all the ratios $e_i/p_i \cdot k$ are simultaneously equal. [22] For example, the Born cross section $d\sigma/\cos\theta_{cm}(u\overline{d} \to W^+\gamma)$ vanishes identically at an angle determined from the ratio of charges: $\cos\theta_{cm} = e_d/e_{W^+} = -1/3$. [24] Such "radiative amplitude zeroes" or "null zones" occur at lowest order in the Standard Model because the electromagnetic spin currents of the quarks and the vector gauge bosons are all canonical.

The vanishing of the forward helicity-flip Compton amplitude at zero energy for the canonical couplings, together with the optical theorem and dispersion theory, leads to a superconvergent sum rule; *i.e.*, a zero value for the DHG sum rule. This remarkable observation was first made for quantum electrodynamics and the electroweak theory by Altarelli, Cabibbo and Maiani. [25] More generally, one can use a quantum loop [26] expansion to show that the logarithmic integral of the spin-

dependent part of the photoabsorption cross section

$$\int_{\nu_{th}}^{\infty} \frac{d\nu}{\nu} \Delta\sigma_{\rm Born}(\nu) = 0 \tag{3}$$

for any $2 \to 2$ Standard Model process $\gamma a \to bc$ in the classical, tree graph approximation. The particles a, b, c and d can be leptons, photons, gluons, quarks, elementary Higgs particles, supersymmetric particles, etc. We also can extend the sum rule to certain virtual photon processes. Here $\nu = p \cdot q/M$ is the laboratory energy and $\Delta\sigma(\nu) = \sigma_P(\nu) - \sigma_A(\nu)$ is the difference between the photoabsorption cross section for parallel and antiparallel photon and target helicities. The sum rule receives nonzero contributions in higher order perturbation theory in the Standard Model from both quantum loop corrections and higher particle number final states. Similar arguments also imply that the DHG integral vanishes for virtual photoabsorption processes such as $\ell\gamma \to \ell Q\overline{Q}$ and $\ell g \to \ell Q\overline{Q}$, the lowest order sea-quark contribution to polarized deep inelastic photon and hadron structure functions. Note that the integral extends to $\nu = \nu_{th}$, which is generally beyond the usual leading twist domain.

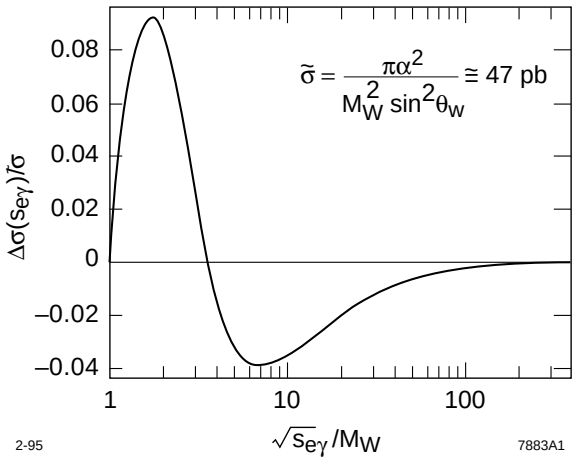

Figure 6: The Born cross section difference $\Delta\sigma$ for the Standard Model process $\gamma e \to W\nu$ for parallel minus antiparallel electron/photon helicities as a function of $\log \sqrt{s}_{e\gamma}/M_W$ The logarithmic integral of $\Delta\sigma$ vanishes in the classical limit.

Schmidt, Rizzo and I [14] have shown that one can use Eq. (3) as a new way to test the canonical couplings of the Standard Model and to isolate the higher order radiative corrections. The sum rule also provides a non-trivial consistency check on calculations of the polarized cross sections. Probably the most interesting application and test of the Standard Model is to the reactions $\gamma\gamma \to q\overline{q}$, $\gamma e \to W\nu$ and $\gamma e \to Ze$ which can be studied in high energy polarized electron-

positron colliders with back-scattered laser beams. In contrast to the timelike process $e^+e^- \to W^+W^-$, the $\gamma\gamma$ and γe reactions are sensitive to the anomalous moments of the gauge bosons at $q^2 = 0$. The cancellation of the positive and negative contributions [27] of $\Delta\sigma(\gamma e \to W\nu)$ to the DHG integral is evident in Fig. 6.

We can also exploit the fact that the vanishing of the logarithmic integral of $\Delta\sigma$ in the Born approximation also implies that there must be a center-of-mass energy, $\sqrt{s}_0$, where the polarization asymmetry $A = \Delta\sigma/\sigma$ possesses a zero, *i.e.*, where $\Delta\sigma(\gamma e \to W\nu)$ reverses sign. [14] We find strong sensitivity of the position of this zero or "crossing point" (which occurs at $\sqrt{s}_{\gamma e} = 3.1583\ldots M_W \simeq 254\,\mathrm{GeV}$ in the SM) to modifications of the SM trilinear γWW coupling. Given reasonable assumptions for the luminosity and energy range for the Next Linear Collider(NLC), the zero point, $\sqrt{s}_0$, of the polarization asymmetry may be determined with sufficient precision to constrain the anomalous couplings of the W to better than the 1% level at 95% CL. Since the zero occurs at rather modest energies where the unpolarized cross section is near its maximum, an electron-positron collider with $\sqrt{s} = 320 - 400$ GeV is sufficient, whereas other techniques aimed at probing the anomalous couplings through the $\gamma e \to W\nu$ process require significantly larger energies. In addition to the fact that only a limited range of energy is required, the polarization asymmetry measurements have the advantage that many of the systematic errors cancel in taking cross section ratios. This technique can clearly be generalized to other higher order tree-graph processes in the Standard Model and supersymmetric gauge theory. The position of the zero in the photoabsorption asymmetry thus provides an additional weapon in the arsenal used to probe anomalous trilinear gauge couplings.

5. Acknowledgments

This work is supported in part by the United States Department of Energy grants DE-AC03-76SF00515 and DE-FG03-96ER40969. Section 2 was written in collaboration with Dave Soper and Francesco Hautmann. Section 3 is based on collaborations with I. Schmidt and T. Rizzo. I also thank C. J., D. Robertson, and A. Pang for helpful conversations.

References

1. For a review, see S. J. Brodsky and P. M. Zerwas, *Nucl. Instrum. Meth.* **A355** *(1995) 19, hep-ph/9407362.*
2. *For a review see V. Telnov, hep-ph/9710014, and these proceedings.*
3. *S. J. Brodsky and G. P. Lepage,* Phys. Rev. Lett. **53**, *545 (1979);* Phys. Lett. **87B**, *359 (1979); G. P. Lepage and S. J. Brodsky,* Phys. Rev. **D22**, *2157 (1980).*
4. *E. Braaten and S.-M. Tse,* Phys. Rev. **D35**, *2255 (1987). F. M. Dittes and A. V. Radyushkin,* Sov. J. Nucl. Phys. **34**, *293 (1981);* Phys. Lett. **134B**, *359 (1984). R. D. Field, R. Gupta, S. Otto and L. Chang,* Nucl. Phys. **B186**, *429 (1981).*
5. *J. Dominick,* et al., *Phys. Rev.* **D50**, *3027 (1994). See also, J. Gronberg* et al. *Phys. Rev.* **D57** *(1998) 33, hep-ex/9707031.*

6. *S. J. Brodsky, C.-R. Ji, A. Pang, and D. Robertson, Phys. Rev.* **D57**, *245 (1998), hep-ph/9705221*
7. *S. J. Brodsky, F. Hautmann and D. E. Soper,* Phys. Rev. **D56**, *6957 (1997), hep-ph/9706427.*
8. *J. Bartels, A. De Roeck, and H. Lotter,* Phys. Lett. **B389**, *742(1996), hep-ph/9608401*
9. *H. Abramowicz, plenary talk at ICHEP96 (Warsaw, July 1996), in Proceedings of the XXVIII International Conference on High Energy Physics, eds. Z. Ajduk and A. K. Wroblewski, World Scientific, p.53.*
10. *L. N. Lipatov,* Sov. J. Nucl. Phys. **23**, *338 (1976); E. A. Kuraev, L. N. Lipatov, and V. S. Fadin,* Sov. Phys. JETP **45**, *199 (1977) ; I. Balitskii and L. N. Lipatov,* Sov. J. Nucl. Phys. **28**, *822 (1978).*
11. *J. D. Bjorken and J. Kogut,* Phys. Rev. **D8**, *1341 (1973).*
12. *J. D. Bjorken, preprint SLAC-PUB-7341, presented at Snowmass 1996 Summer Study on New Directions for High Energy Physics, hep-ph/9610516.*
13. *A. H. Mueller,* Nucl. Phys. **B437**, *107 (1995).*
14. *S. J. Brodsky, T. Rizzo and I. Schmidt,* Phys. Rev. **D52, 4929** *(1995), hep-ph/9505441*
15. *S. Weinberg, Lectures on elementary particles and field theory, Vol. 1, eds. S. Deser, M. Grisaru and H. Pendleton (MIT Press, 1970, Cambridge, USA).*
16. *S. Ferrara, M. Porrati, and V. L. Telegdi,* Phys. Rev. **D46**, *3529 (1992).*
17. *S. D. Drell and A. C. Hearn,* Phys. Rev. Lett. **16**, *908 (1966); S. Gerasimov,* Yad. Fiz. **2**, *598 (1965) [*Sov. J. Nucl. Phys. **2**, *430 (1966)]; L. I. Lapidus and Chou Kuang-Chao,* J. Exptl. Theoretical Physics **41**, *1545 1961) [*Sov. Phys. JETP **14**, *1102 (1962)]; M. Hosada and K. Yamamoto,* Prog. Theor. Phys. **36**, *426 (1966). For reviews of the empirical tests of the DHG sum rule see B. L. Ioffe, preprint ITEP-61 (1994) hep-ph/9408291, and D. Drechsel,* Prog. Part. Nucl. Phys. **34**, *181 (1995), nucl-th/9411034*
18. *S. J. Brodsky, S. D. Drell,* Phys. Rev. **D22**, *2236 (1980). For a review of the empirical bounds on the radii and the anomalous moments of leptons and quarks, see G. Köpp, D. Schaile, M. Spira, and P. M. Zerwas,* Z. Phys. **C65**, *545 (1995), hep-ph/9409457*
19. *S. J. Brodsky and F. Schlumpf,* Phys. Lett. **B329**, *111 (1994), and* Phys. Lett. **B360,** *1 (1995), hep-ph/9505276.*
20. *S.J. Brodsky and J. R. Hiller,* Phys. Rev. **D46**, *2141 (1992).*
21. *V. Bargmann, L. Michel, and V. L. Telegdi,* Phys. Rev. Lett. **2**, *435 (1959).*
22. *R. W. Brown, K. L. Kowalski and S. J. Brodsky,* Phys. Rev. **D28**, *624 (1983); S. J. Brodsky and R. W. Brown,* Phys. Rev. Lett. **49**, *966 (1982).*
23. *F. E. Low,* Phys. Rev. **96**, *1428 (1954);* Phys. Rev. **110**, *974 (1958). M. Gell-Mann and M. L. Goldberger,* Phys. Rev. **96**, *1433 (1954).*
24. *K. O. Mikaelian, M. A. Samuel and D. Sahdev,* Phys. Rev. Lett. **43**, *746 (1979).*
25. *G. Altarelli, N. Cabibbo, and L. Maiani,* Phys. Lett. **40**, *415 (1972).*
26. *S. J. Brodsky and I. A. Schmidt,* Phys. Lett. **B351**, *344 (1995), hep-ph/9502416*
27. *I. F. Ginzburg, G. L. Kotkin, S. L. Panfil and V. G. Serbo,* Nucl. Phys. **B228**, *285 (1983). See also S. Y. Choi and F. Schrempp,* Phys. Lett. **B272**, *149 (1991); M. Raidal,* Nucl. Phys. **B441**, *49 (1995), hep-ph/9411243 .*